Available online at www.sciencedirect.com

ScienceDirect

IFAC PapersOnline CONFERENCE PAPER ARCHIVE

IFAC PapersOnLine 55-12 (2022) 214–221

Photovoltaic System's MPPT Under Partial Shading Using T-S Fuzzy Robust Control

Redouane Chaibi[a], Rachid EL Bachtiri[a], Karima El Hammoumi[a] Mohamed Yagoubi[b]

[a] *Industrial Technologies and Services Laboratory, Higher School of Technology, Sidi Mohamed Ben Abdellah University, Fez 30000, Morocco (e-mail: c.redouane.chaibi@gmail.com {rachid.elbachtiri;karima.elhammoumi}@usmba.ac.ma).*

[b] *IMT Atlantique, LS2N (UMR CNRS 6004), Nantes, France. (e-mail: mohamed.yagoubi@imt-atlantique.fr)*

Abstract: This paper deals with a T-S fuzzy robust control achieving maximum power point tracking (MPPT) for photovoltaic (PV) systems under partial shading situations. The aim is to track global maximum power point (GMPP). The T-S fuzzy robust control consists in an optimization approach that overcomes the well-known perturb and observe (P&O) technique drawbacks, such as the decreased tracking efficiency and transient oscillations. For this aim, a photovoltaic generator (PVG) with a DC-DC boost converter and battery energy storage devices are considered. The optimum trajectory is generated using a T-S fuzzy reference model, which must be followed to obtain optimal powerpoint. Solving a set of linear matrix inequalities (LMIs) yields the sought controller gains. A simulation is carried out to show that the tracking performance of the proposed T-S fuzzy robust control is assessed for various partial shading patterns. The results confirm that the T-S fuzzy robust H_∞ control strategy ensures global MPP convergence. Furthermore, when compared to the existing solutions, simulations proved that it has better performances.

Keywords: Photovoltaic system; partial shading conditions (PSCs); Batteries; Boost converter; Maximum power point traking; Takagi-Sugeno fuzzy systems.

1. INTRODUCTION

Global demand for the use of renewable energies has sparked a lot of interest due to rising energy needs and environmental concerns. Photovoltaic (PV) power systems are one of the most extensively used renewable energy sources. Nonetheless, several challenges must be addressed before these technologies may be deployed. One of the most pressing challenge is how to improve the efficiency of solar panels Bosman et al. (2020), Al-Shahri et al. (2021). Several maximum power point tracking (MPPT) algorithms have been developed to extract maximum power from the PV system. The goal of MPPT is to optimize and improve the use of photovoltaic systems, as well as to increase array efficiency to ensure maximum power generation Mekhilef et al. (2012), Solangi et al. (2011). So far, many MPPT approaches have been established. Open-circuit voltage Dorofte et al. (2005), short circuit current Noguchi et al. (2002), perturb and observe (P&O) method Kumar et al. (2017), incremental conductance (INC) method Mei et al. (2010), and others are among these approaches. Standard MPPT approaches differ in terms of convergence speed, the number of sensors employed and the system cost Esram and Chapman (2007). The P&O approach is a straightforward MPPT methodology Esram and Chapman (2007). It is hence the most extensively used algorithm due to its ease of implementation. The main weaknesses of this strategy are the occurrence of oscillations around the MPP, as well as its limited ability to track this point under changing environmental conditions. The INC method Motahhir et al. (2018) was presented to reduce these oscillations and improve system efficiency, however, oscillations were not eliminated. In addition, most MPPT approaches assume that all cells in a module receive the same irradiation. On the other hand, PV modules are frequently exposed to partial shadow conditions (PSC), which is the primary cause of output power decrease Woyte et al. (2003), Chouder and Silvestre (2009), Armstrong and Hurley (2010). Under partial shading conditions (PSCs), when the PV cells do not receive uniform irradiance, the P-V curve exhibits many power maxima peaks, and as a result, techniques like (P&O and INC) frequently fail to find the global maximum power point (GMPP) because they converge to the MPP that makes contact first, which is likely one of the local maximum power points (LMPPs). This leads to significant energy waste Shenoy et al. (2012), Alonso et al. (2009). To obtain the available optimum power from the PV array under PSCs, an intelligent and efficient MPPT approach is necessary to operate PV systems at the GMPP. Particle Swarm Optimisation (PSO), suggested by authors in Eberhart and Kennedy (1995), is a bio-inspired algorithm

10.1016/j.ifacol.2022.07.314

that was created after studying the social and cognitive behavior of birds. The PSO method is used to monitor the Global Point (GP), particularly in partial shading conditions Phimmasone et al. (2013), Miyatake et al. (2007). The beginning location of the agents has a substantial impact on PSO convergence, resulting in a low convergence rate in some cases. Furthermore, PSO based methods require the determination of five parameters, making them complicated. As a result, studying PV non-linearity under various weather situations is still a challenging issue. Therefore, this work proposes the use of Takagi-Sugeno (T-S) models that are increasing in popularity since they can efficiently incorporate a large range of nonlinear systems Takagi and Sugeno (1985). Numerous important results have already been suggested using this formalism Chaibi et al. (2020, 2021). In Chang and Yang (2010); Chaibi et al. (2019), adequate LMI criteria are determined to ensure the overall stability. To increase MPP tracking capacity during fast-changing irradiance levels, a few improved T-S fuzzy controllers have been developed Zayani et al. (2015), Allouche et al. (2018b) in which the ideal trajectory was generated using a T-S reference model. In addition, a MPPT T-S fuzzy controller for a PV system with battery storage under varying meteorological conditions is proposed in El Hammoumi et al. (2022). On the other hand, the previous studies, do not address the scenario of shading, in which the PV cells do not get uniform insolation and the P-V curve has several maximum power peaks. Thus, to collect the optimal power available from the PV array under PSCS, an efficient MPPT approach is required to run PV systems at GMPP. The goal of this study is to identify the global peak during PSCs, and to address some of the issues that have occurred, such as poorer tracking efficiency and oscillations in PV output power. To properly track the MPP of PV systems with battery storage, the Lyapunov function is employed to establish suitable circumstances for the existence of a T-S fuzzy robust control. As a consequence, the control is obtained by solving a set of LMIs. The suggested fuzzy robust control uses an H_∞ performance controller to attenuate perturbation effects and provides high-efficiency tracking of GMPP corresponding to different PSCs.

2. PV CELL MODELING AND PARTIAL SHADING CONDITION

2.1 The fundamental properties of a PV cell

The boost converter is coupled between the solar panel and a battery load. The suggested PV system design is depicted in Fig. 1.

2.2 Modeling of the PV generator

The PV cell equivalent circuit is depicted in Fig.2. The model contains a current source, a diode, and resistances.

The following equation may be used to determine the PV array's electrical characteristics:

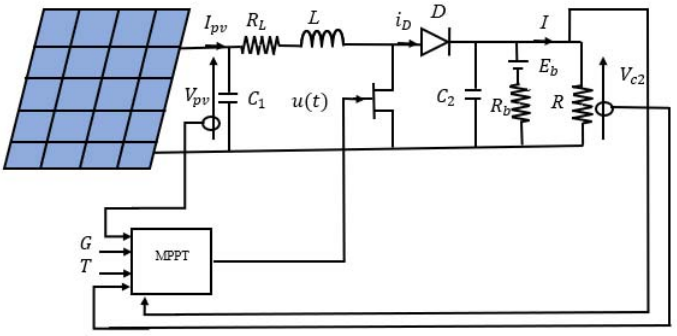

Fig. 1. Global structure of the PV system

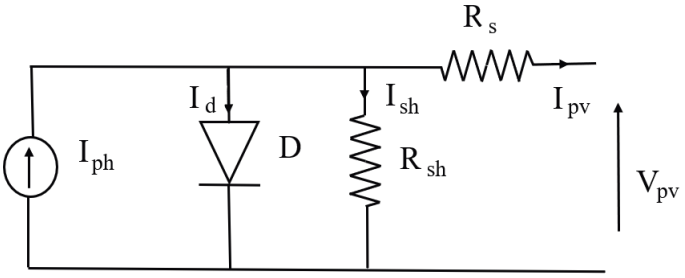

Fig. 2. Equivalent circuit model of the PV cell.

$$I_{pv} = I_{ph} - I_d - I_{sh} = I_{ph} - I_0\left[exp(\frac{V_{pv} + R_s I_{pv}}{nV_T}) - 1\right] - \left(\frac{V_{pv} + R_s I_{pv}}{R_{sh}}\right) \quad (1)$$

where

$$V_T = \frac{KT}{q}$$

$$I_{ph} = [I_{scr} + K_i(T - T_r)]\left(\frac{G}{1000}\right) \quad (2)$$

The short-circuit current at a reference state and the short-circuit temperature coefficient are denoted by I_{scr} and K_i, respectively. T_r and G are respectively the reference temperature and the solar irradiance (W/m^2). $K = 1.3805 \times 10^{-23} J/K$, $q = 1.6 \times 10^{-19} C$ represents the Boltzmann's constant and the electronic charge respectively. R_s is the series resistance of the cell and R_{sh} is the parallel resistance of the cell. The saturation current of a diode is represented by I_0. I_{ph} represents the generated photocurrent. T, V_{pv} and I_{pv} represent the cell temperature the output voltage, and the output current, of the PV module respectively. The mathematical model for a PV module constructed of N_p parallel connection is expressed by the following equation:

$$I_{pv} = N_p I_{ph} - N_p I_0\left[exp(\frac{V_{pv} + R_s I_{pv}}{nV_T}) - 1\right] - N_p\left(\frac{V_{pv} + R_s I_{pv}}{N_s R_{sh}}\right) \quad (3)$$

where N_S is the number of cells in series per string.

2.3 Effect of partial shading on PV array

Large numbers of solar panels are connected in a series/parallel configuration for maximum power. P-V curves

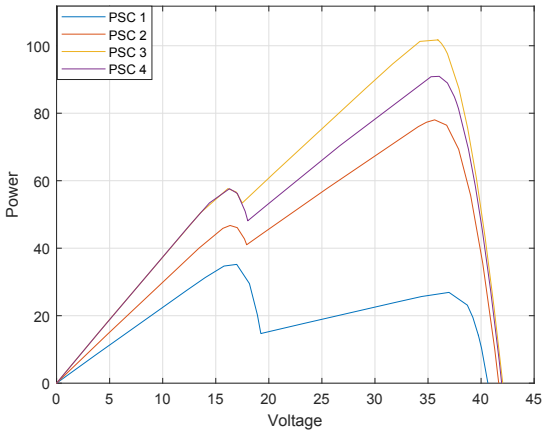

Fig. 3. P-V curves under non-uniform irradiance

contain just one maximum power point when all solar panels get the same irradiance levels. However, irradiance levels fluctuate dramatically owing to changes in weather conditions or variables such as shade from buildings and clouds. So irradiance levels become non-uniform which causes several peaks in P-V curves, as illustrated in Fig.3. There is only one global maximum (GM), although there are several local maxima (LM). To extract this GM from many LMs, a complex MPPT control is necessary.

2.4 DC–DC Boost converter

Two linear differential equations, depending on switcher position, describe the dynamic behavior of the entire boost converter circuit coupled to the battery load. To simplify the process, we will establish the MPPT control when the battery is completely charged. During the 'ON' state, the differential equation of a DC–DC boost converter may be defined by (see Allouche et al. (2018a)):

$$\begin{cases} \dfrac{dV_{pv}(t)}{dt} = -\dfrac{1}{C_1}(I_L(t) - I_{PV}(t)) \\ \dfrac{dI_L(t)}{dt} = \dfrac{1}{L}V_{pv}(t) - \dfrac{R_L}{L}I_L(t) \\ \dfrac{dV_{c2}(t)}{dt} = -\dfrac{1}{RC_2}V_{c2}(t) \end{cases} \tag{4}$$

We also have the following equalities during the 'OFF' period.

$$\begin{cases} \dfrac{dV_{pv}(t)}{dt} = -\dfrac{1}{C_1}(I_L(t) - I_{PV}(t)) \\ \dfrac{dI_L(t)}{dt} = \dfrac{1}{L}V_{pv}(t) - \dfrac{R_L}{L}I_L(t) - \dfrac{1}{L}V_{c2}(t) \\ \dfrac{dV_{c2}(t)}{dt} = \dfrac{1}{C_2}I_L(t) - \dfrac{1}{RC_2}V_{c2}(t) \end{cases} \tag{5}$$

where I_L , V_{PV}, and V_{c2} indicate inductor current, input voltage and output voltage, respectively.
During the 'ON 'period, the state-space equation is described as follows:

$$\dot{x}(t) = A_1 x(t) + E\omega(t) \tag{6}$$

And the state-space equation during the 'OFF' period is given by the following equation

$$\dot{x}(t) = A_2 x(t) + E\omega(t) \tag{7}$$

Where,

$$A_1 = \begin{bmatrix} 0 & -\dfrac{1}{C_1} & 0 \\ \dfrac{1}{L} & -\dfrac{R_L}{L} & 0 \\ 0 & 0 & -\dfrac{1}{RC_2} \end{bmatrix}, \quad A_2 = \begin{bmatrix} 0 & -\dfrac{1}{C_1} & 0 \\ \dfrac{1}{L} & -\dfrac{R_L}{L} & -\dfrac{1}{L} \\ 0 & \dfrac{1}{C_2} & -\dfrac{1}{RC_2} \end{bmatrix}$$

$$E = \begin{bmatrix} \dfrac{1}{C_1} \\ 0 \\ 0 \end{bmatrix}, \quad x(t) = \begin{bmatrix} V_{pv}(t) \\ I_L(t) \\ V_{c2}(t) \end{bmatrix}, \quad \omega(t) = I_{pv}(t)$$

So, the dynamics of the PV system can be rewritten as:

$$\dot{x}(t) = [A_1 x(t) + E\omega(t)]u(t) + [A_2 x(t) + E\omega(t)](1 - u(t)) \tag{8}$$

Or equally,

$$\dot{x}(t) = A_2 x(t) + (A_1 - A_2)x(t)u(t) + E\omega(t) \tag{9}$$

As well,

$$\dot{x}(t) = A_2 x(t) + B(x(t))u(t) + E\omega(t) \tag{10}$$

with $u(t) \in [0, 1]$ indicates the duty ratio employed as an input to control the power switch, and

$$B(x(t)) = \begin{bmatrix} 0 \\ \dfrac{V_{c2}(t)}{L} \\ -\dfrac{I_L(t)}{C_2} \end{bmatrix}$$

3. T–S FUZZY CONTROL

Based on the T–S fuzzy control scheme, the duty cycle of the DC–DC boost converter can be determined, which allows the photovoltaic generator to operate very close to its maximum power trajectory for any change in solar insolation or temperature.

3.1 T-S Fuzzy model for the boost converter

T-S fuzzy systems can adequately represent the PV system, thanks to their ability to transform higher-order nonlinear systems into a weighted combination of a set of linear systems. So, according to the dynamic model proposed in Allouche et al. (2018b), the T-S fuzzy functions for total membership are configured as follows:

$$\begin{cases} \sigma_1(t) = V_{c2}(t) \\ \sigma_2(t) = I_L(t) \end{cases} \tag{11}$$

Following the techniques described in Allouche et al. (2018b), the membership functions of the T-S fuzzy model may be derived as follow:

$$\eta_{1,min}(\sigma(t)) = \frac{\sigma_1(t) - \sigma_{1,min}}{\sigma_{1,max} - \sigma_{1,min}}$$
$$\eta_{1,max}(\sigma(t)) = 1 - \eta_{1,min}(\sigma(t))$$
$$\eta_{2,min}(\sigma(t)) = \frac{\sigma_2(t) - \sigma_{2,min}}{\sigma_{2,max} - \sigma_{2,min}}$$
$$\eta_{2,max}(\sigma(t)) = 1 - \eta_{2,min}(\sigma(t))$$

The weighting functions h_i employed have the following expressions :

$$h_1(\sigma(t)) = \eta_{1,min}(\sigma(t))\eta_{2,min}(\sigma(t))$$
$$h_2(\sigma(t)) = \eta_{1,min}(\sigma(t))\eta_{2,max}(\sigma(t))$$
$$h_3(\sigma(t)) = \eta_{1,max}(\sigma(t))\eta_{2,min}(\sigma(t))$$
$$h_4(\sigma(t)) = \eta_{1,max}(\sigma(t))\eta_{2,max}(\sigma(t))$$

The PV system is described by the following four fuzzy rules:

Rule 1: If ($V_{c2}(t)$ is $\eta_{1,min}$) and ($I_L(t)$ is $\eta_{2,min}$) Then
$$\dot{x} = A_2x(t) + B_1u(t) + E\omega(t)$$

Rule 2: If ($V_{c2}(t)$ is $\eta_{1,min}$) and ($I_L(t)$ is $\eta_{2,max}$) Then
$$\dot{x} = A_2x(t) + B_2u(t) + E\omega(t)$$

Rule 3: If ($V_{c2}(t)$ is $\eta_{1,max}$) and ($I_L(t)$ is $\eta_{2,min}$) Then
$$\dot{x} = A_2x(t) + B_3u(t) + E\omega(t)$$

Rule 4: If ($V_{c2}(t)$ is $\eta_{1,max}$) and ($I_L(t)$ is $\eta_{2,max}$) Then
$$\dot{x} = A_2x(t) + B_4u(t) + E\omega(t)$$

$$B_1 = \begin{bmatrix} 0 \\ \frac{V_{c2min}(t)}{L} \\ -\frac{I_{Lmin}(t)}{C_2} \end{bmatrix}, \quad B_2 = \begin{bmatrix} 0 \\ \frac{V_{c2min}(t)}{L} \\ -\frac{I_{Lmax}(t)}{C_2} \end{bmatrix},$$

$$B_3 = \begin{bmatrix} 0 \\ \frac{V_{c2max}(t)}{L} \\ -\frac{I_{Lmin}(t)}{C_2} \end{bmatrix}, \quad B_4 = \begin{bmatrix} 0 \\ \frac{V_{c2max(t)}}{L} \\ -\frac{I_{Lmax}(t)}{C_2} \end{bmatrix}$$

The T-S fuzzy model may be written as follows:

$$\dot{x}(t) = \sum_{i=1}^{4} h_i(\sigma(t))(A_2x(t) + B_iu(t) + E\omega(t)) \tag{12}$$

Moreover note that the following lemma is needed for the construction of fuzzy controllers.

Lemma 1. Chang et al. (2015) For matrices T, Q, U, and W with appropriate dimensions and scalar ξ, the inequality
$$T + W^TQ^T + QW < 0 \tag{13}$$
is fulfilled if the following condition holds:
$$\begin{bmatrix} T & * \\ \xi Q^T + UW & -\xi U - \xi U^T \end{bmatrix} < 0$$

3.2 MPPT reference model

In this section, the objective is to design a fuzzy system, that can follow a perfect reference model. The MPP reference model can be expressed as:

$$\dot{x}_r(t) = A_rx_r(t) + r(t) \tag{14}$$

where,

$$A_r = \begin{bmatrix} 0 & -\frac{1}{C_1} & 0 \\ \frac{1}{L} & -\frac{R_L}{L} & -\frac{1}{L}(1-u_{opt}) \\ 0 & \frac{1}{C_2}(1-u_{opt}) & -\frac{1}{RC_2} \end{bmatrix},$$

$$r(t) = \begin{bmatrix} \frac{I_{pvopt}}{C_1} \\ 0 \\ 0 \end{bmatrix}, \quad u_{opt} = \sqrt{\frac{V_{pvopt}}{RI_{pvopt}}}$$

The reference model (14) is also nonlinear via the premise variable $\sigma_r := (1 - u_{opt})$, and can be characterized by the following two rules:

Rule 1 : If($\sigma_r(t)$ is N_{min}) Then $\dot{x}_r(t) = A_{r1}x_r(t) + r(t)$

Rule 2 : If($\sigma_r(t)$ is N_{max}) Then $\dot{x}_r(t) = A_{r2}x_r(t) + r(t)$

The membership and weighting functions are defined as follows:

$$h_1(\sigma_r(t)) = N_{min}(\sigma_r(t)) = \frac{\sigma_r(t) - \sigma_{r,min}}{\sigma_{r,max} - \sigma_{r,min}}$$
$$h_2(\sigma_r(t)) = N_{max}(\sigma_r(t)) = 1 - h_1(\sigma_r(t))$$

The matrices of the reference model are defined as:

$$A_{r1} = \begin{bmatrix} 0 & -\frac{1}{C_1} & 0 \\ \frac{1}{L} & -\frac{R_L}{L} & -\frac{1}{L}\sigma_{r,min} \\ 0 & \frac{1}{C_2}\sigma_{r,min} & -\frac{1}{RC_2} \end{bmatrix},$$

$$A_{r2} = \begin{bmatrix} 0 & -\frac{1}{C_1} & 0 \\ \frac{1}{L} & -\frac{R_L}{L} & -\frac{1}{L}\sigma_{r,max} \\ 0 & \frac{1}{C_2}\sigma_{r,max} & -\frac{1}{RC_2} \end{bmatrix},$$

The T–S fuzzy reference model may be described as follows:

$$\dot{x}_r(t) = \sum_{k=1}^{2} h_k(\sigma_r(t))(A_{rk}x_r(t) + r(t)) \tag{15}$$

3.3 Fuzzy controller design

We need to ensure that the tracking error $e(t) = x(t) - x_r(t)$ converges to zero regardless of weather variation in order to keep operating at the maximum power point. As a result, the problem of trajectory tracking is represented as a fuzzy state-feedback control, with a control law of the form :

$$\begin{aligned} u(t) &= \sum_{j=1}^{4} h_j(\sigma(t))K_j(x(t) - x_r(t)) \\ &= \sum_{j=1}^{4} h_j(\sigma(t))K_je(t) \end{aligned} \tag{16}$$

where K_j are linear feedback gain matrices to be developed. The following equations may be used to determine the tracking dynamics error of the systems (12), (15), and (16) :

$$\begin{aligned} \dot{e}(t) = \sum_{i=1}^{4}\sum_{j=1}^{4}\sum_{k=1}^{2} h_i(\sigma(t))h_j(\sigma(t))h_k(\sigma_r(t)) \\ [(A_2 + B_iK_j)e(t) + (A_2 - A_{rk})x_r(t) + E\omega(t) - r(t)] \end{aligned} \tag{17}$$

Substituting the control law (16) in the fuzzy model (12) and using an augmented state-space form, the closed-loop system is given by:

$$\begin{aligned} \dot{\bar{x}}(t) = \sum_{i=1}^{4}\sum_{j=1}^{4}\sum_{k=1}^{2} h_i(\sigma(t))h_j(\sigma(t))h_k(\sigma_r(t)) \\ [\bar{A}_{ijk}\bar{x}(t) + \bar{E}\bar{\omega}(t)] \end{aligned} \tag{18}$$

Where,

$$\bar{x}(t) = \begin{bmatrix} e(t) \\ x_r(t) \end{bmatrix}, \quad \bar{\omega}(t) = \begin{bmatrix} \omega(t) \\ r(t) \end{bmatrix}, \quad \bar{E}(t) = \begin{bmatrix} E & -I \\ 0 & I \end{bmatrix},$$

$$\bar{A}_{ijk} = \begin{bmatrix} A_2 + B_iK_j & A_2 - A_{rk} \\ 0 & A_{rk} \end{bmatrix},$$

where, $\omega(t)$ represents the disturbance caused by input voltage variation, including parameters (I_{pvopt} and I_{pv}), and $r(t)$ represents the external input, which is dependent on climatic conditions.

To rapidly reduce the influence of disturbances on the closed-loop system, a H_∞ performance may be expressed as follows:

$$\int_0^\infty \bar{x}(t)\bar{Q}\bar{x}(t)dt \leq \gamma^2 \int_0^\infty \bar{\omega}^T(t)\bar{\omega}(t)dt \tag{19}$$

where, $\bar{Q} = \begin{bmatrix} Q_1 & 0 \\ 0 & 0 \end{bmatrix}$, Q_1 is a weighting matrix to be tuned.

It is now possible to present sufficient conditions for the existence of a T–S fuzzy controller (16) that will ensure that the PV generator is operating very close to the maximum power trajectory. Based on the above analysis, we obtained this Theorem which reduces the maximum power tracking error when climatic conditions change.

Theorem 1. Given positive scalars α and ξ the closed-loop system (18) is asymptotically stable and the H_∞ performance (19) with the attenuation level γ is satisfied, if there are some matrices $P_1 > 0$, $P_2 > 0$, P_3, U, N_i, $i = 1, ...4$ and a positive scalar γ solution for the following optimization problem:

$$\Psi_{iik} < 0, \quad k = 1, 2 \tag{20}$$

$$\Psi_{ijk} + \Psi_{jik} < 0, \quad k = 1, 2 \tag{21}$$

Where,

$$\Psi_{ijk} = \begin{bmatrix} \Psi_{ijk}^{11} & \Psi_{ijk}^{12} & P_1E & P_2 - P_1 & \Psi_{ijk}^{15} \\ * & \Psi_{ijk}^{22} & P_2E & P_3 - P_2 & \Psi_{ijk}^{25} \\ * & * & -\gamma^2 I & 0 & 0 \\ * & * & * & -\gamma^2 I & 0 \\ * & * & * & * & -\xi U - \xi U^T \end{bmatrix} \tag{22}$$

$$\begin{aligned} \Psi_{ijk}^{11} &= sym\{P_1A_2 + B_iN_j\} + Q_1 + \alpha P_1 \\ \Psi_{ijk}^{12} &= P_1(A_2 - A_{rk}) + P_2A_{rk} + (A_2^TP_2 + \lambda N_j^TB_i^T) + \alpha P_2 \\ \Psi_{ijk}^{15} &= \xi(P_1B_i - B_iU) + N_j^T \\ \Psi_{ijk}^{22} &= sym\{P_2(A_2 - A_{rk}) + P_3A_{rk}\} + \alpha P_3 \\ \Psi_{ijk}^{25} &= \xi(P_2B_i - \lambda B_iU) \end{aligned} \tag{23}$$

Furthermore, the controller gain matrices are given by $K_j = U^{-1}N_j$, $j = 1, 2, ..., r$.

4. RESULTS AND DISCUSSION

To evaluate the performance of the MPPT T-S fuzzy controller, the 120 W PV system illustrated in Fig.4 is used. This system includes a PV array consisting of two 60 W PV modules that are serially coupled, as well as a boost DC–DC converter that connects the PV system to the storage system. The elements for the suggested converter employed in simulation are $C_1 = 425\mu F$, $L = 21mH$, $R_l = 0.001\Omega$, $R = 80\Omega$, $C_2 = 416\mu F$. The storage device is a PowerSafe T–S series lead-acid battery. The behavior of the battery linked to the PV system controlled by the fuzzy T–S controller was also visible in this simulation. The SOC profile for PSCs is seen in Figs. 11-13, where I_b signifies the battery current and V_b denotes voltage, with $I_b < 0$ during charging and $I_b > 0$ during discharge. The irradiation parameters used in the simulation testing are shown in Table 3. In Fig. 3, the P-V characteristic achieved in each test is shown. As seen in this figure, the P-V curve under PSCs includes numerous peaks. Each of these peaks has its own voltage and intensity. The number of darkened panels determines the number of peaks. We achieve the minimal

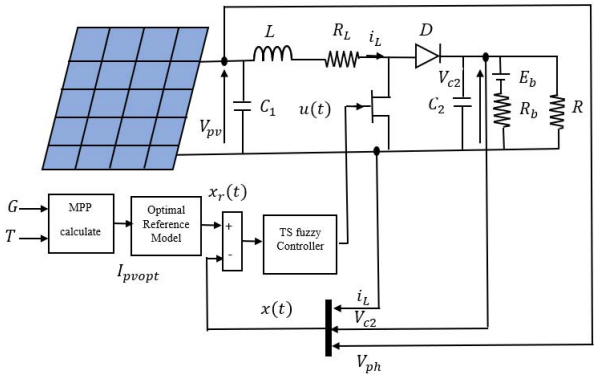

Fig. 4. PV system with MPPT fuzzy structure.

Table 1. $MSX60$ PV module

Parameters	Abbreviation	Value
Maximum power	P_{pvopt}	60 W
Maximum current	I_{pvopt}	3.5A
Maximum voltage	V_{pvopt}	17.1V
Short circuit current	I_{ph}	3.8A
Open circuit voltage	V_{oc}	21.1V

Table 2. Lead acid battery parameters.

Parameters	Name	Value
C	Nominal capacity	$200Ah$
R_{Bat}	Internal resistor	$0.64 \times 12(7.68m\Omega)$
E_{Bat}	Nominal voltage	$2 \times 12V(24V)$

H_∞ disturbance attenuation level $\gamma_{min} = 0.14$, and the following controller gains by solving the LMI conditions in the Theorem 1.

$$\begin{aligned} K_1 &= [-0.0020 \;\; 0.1151 \;\; 0.0839], \\ K_2 &= [-0.0011 \;\; 0.0092 \;\; -0.0039], \\ K_3 &= [-0.0110 \;\; -0.0566 \;\; 0.0109], \\ K_4 &= [-0.0021 \;\; 0.0034 \;\; -0.0029] \end{aligned}$$

Table 3. These irradiation levels were taken into account during simulation testing

Conditions	W/m^2	W/m^2
STC	1000	1000
PSC1	200	600
PSC2	600	800
PSC3	700	1000
PSC4	800	1000

The PV system was simulated using multiple PSCs (PSC1, PSC2, PSC3, and PSC4) in addition to the usual test condition to assess the ability of the MPPT T-S fuzzy controller to monitor the GMPP (STC). The system was first tested under STC, then each PSC was installed. Fig. 5-9 show the obtained results. During PSC 1, the T-S fuzzy controller obtains the global peak (GP) of 35 W, PSO reaches the GP of 34.5 W, and the P&O algorithm only reaches the LP of 34.3 W. The T-S fuzzy controller

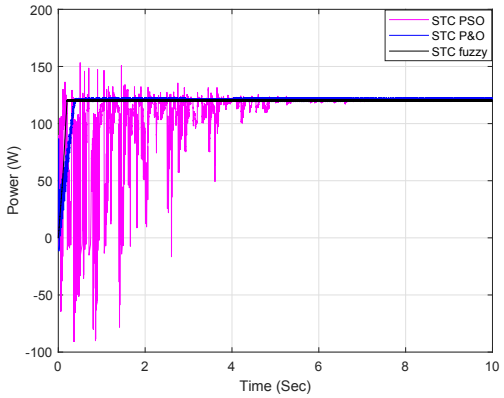

Fig. 5. P-V characteristic curve of the three STC.

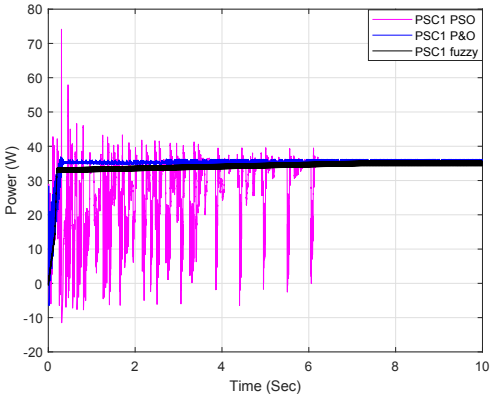

Fig. 6. P-V characteristic curve in case PSC1

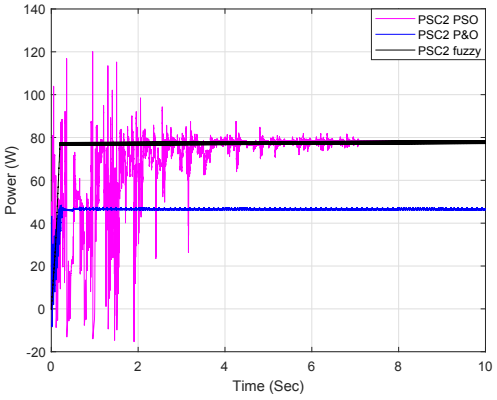

Fig. 7. P-V characteristic curve in case PSC2

reaches the GP of 77.6 W, the PSO reaches the GP of 77.5 W, and the P&O converges to an LP of 46.32 W in PSC 2. Furthermore, when PCS 3 is used, the T-S fuzzy controller reaches the GP of 102.3 W, the PSO meets the GP of 102.2 W, and the P&O reaches the GP of 57.5 W. As a consequence, it is evident that P&O is unable to distinguish between LP and GP.

Throughout the profile, the achieved power of the T-S Fuzzy control is greater than that achieved thanks to PSO and P&O algorithms. The tracking efficiency of PV system output power under various PSC employing P&O, PSO, and T-S Fuzzy control is shown in Fig.6-8. It is possible

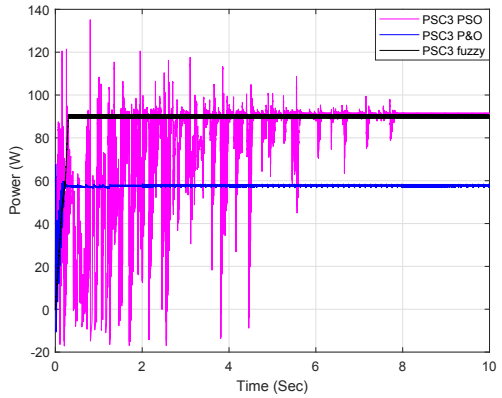

Fig. 8. P-V characteristic curve in case PSC3

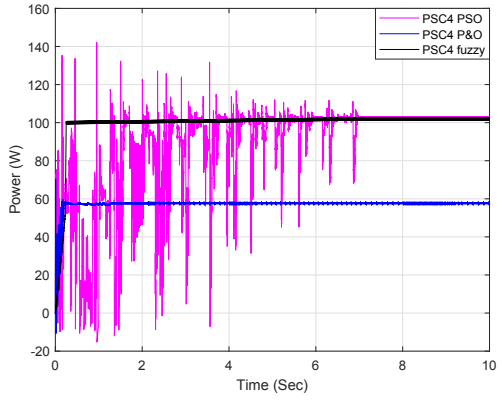

Fig. 9. P-V characteristic curve in case PSC4

to infer that the suggested Fuzzy-MPPT guarantees the tracking of GMPP with higher efficiency than P&O and PSO. The suggested technique clearly outperforms the PSO algorithm in terms of tracking speed. Despite the fact that the P&O algorithm has a faster tracking speed than PSO. In most situations of PSC, the P&O algorithm is unable to monitor the GMPP and is trapped in the local MPP of the P-V curve (in the case of PSC1 and PSC2). When compared to PSO and P&O based MPPT, the T-S Fuzzy control-based MPPT converges with a good speed and less oscillation around the GP.

The second simulation tries to demonstrate the effect of the PSC on the battery's state of charge and discharge. Figs.10-13 depict the battery storage voltage (V_b) and current (I_b) for various PSCs. It should be mentioned that the battery's state of charge (SOC) fluctuates significantly with the intensity of the irradiance. The ability of the MPPT technique to follow the PSC influences the SOC curves.

5. CONCLUSIONS

This paper presents a T-S fuzzy robust control strategy for PV systems that are partially shaded. Solving a set of LMI conditions yields a robust controller enabling to track the global maximum power point. The simulations, undertaken under a variety of partial shade settings as well as some uniform conditions, demonstrate that the proposed technique outperforms existing methods (such as

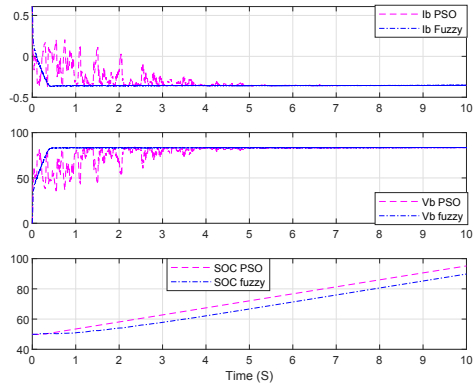

Fig. 10. The battery charge curve in case of STC

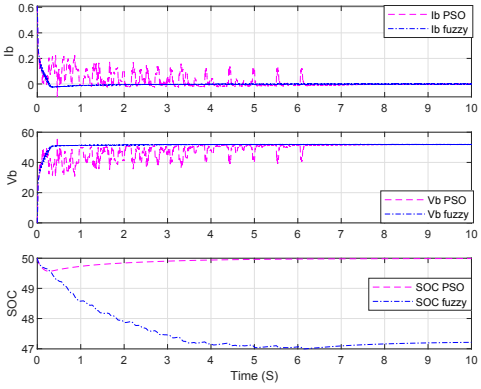

Fig. 11. The battery charge curve in case of PSC1

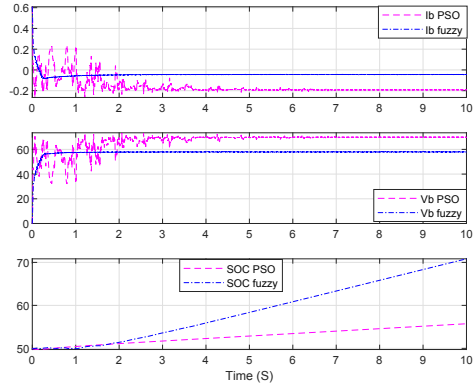

Fig. 12. The battery charge curve in case of PSC2

P&O and PSO based ones) in terms of tracking efficiency and reaction time .

REFERENCES

Al-Shahri, O.A., Ismail, F.B., Hannan, M., Lipu, M.H., Al-Shetwi, A.Q., Begum, R., Al-Muhsen, N.F., and Soujeri, E. (2021). Solar photovoltaic energy optimization methods, challenges and issues: A comprehensive review. *Journal of Cleaner Production*, 284, 125465.

Allouche, M., Dahech, K., and Chaabane, M. (2018a). Multiobjective maximum power tracking control of photovoltaic systems: Ts fuzzy model-based approach. *Soft Computing*, 22(7), 2121–2132.

Allouche, M., Dahech, K., Chaabane, M., and Mehdi, D. (2018b). Fuzzy observer-based control for maximum power-point tracking of a photovoltaic system. *International Journal of Systems Science*, 49(5), 1061–1073.

Alonso, R., Ibanez, P., Martinez, V., Roman, E., and Sanz, A. (2009). An innovative perturb, observe and check algorithm for partially shaded pv systems. In *2009 13th European Conference on Power Electronics and Applications*, 1–8. IEEE.

Armstrong, S. and Hurley, W. (2010). A thermal model for photovoltaic panels under varying atmospheric conditions. *Applied thermal engineering*, 30(11-12), 1488–1495.

Bosman, L.B., Leon-Salas, W.D., Hutzel, W., and Soto, E.A. (2020). Pv system predictive maintenance: Challenges, current approaches, and opportunities. *Energies*, 13(6), 1398.

Chaibi, R., El Aiss, H., El Hajjaji, A., and Hmamed, A. (2020). Stability analysis and robust h_∞ controller synthesis with derivatives of membership functions for ts fuzzy systems with time-varying delay: Input-output stability approach. *International Journal of Control, Automation and Systems*, 18(7), 1872–1884.

Chaibi, R., Er Rachid, I., Tissir, E.H., and Hmamed, A. (2019). Finite-frequency static output feedback h_∞ control of continuous-time t–s fuzzy systems. *Journal of Circuits, Systems and Computers*, 28(02), 1950023.

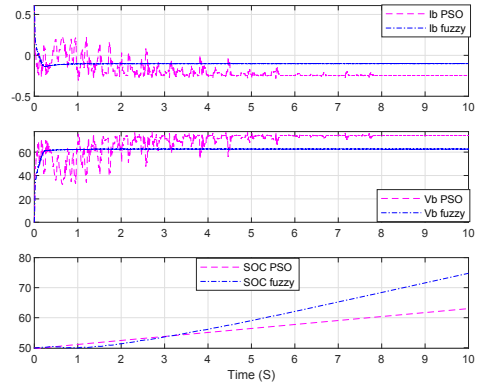

Fig. 13. The battery charge curve in case of PSC3

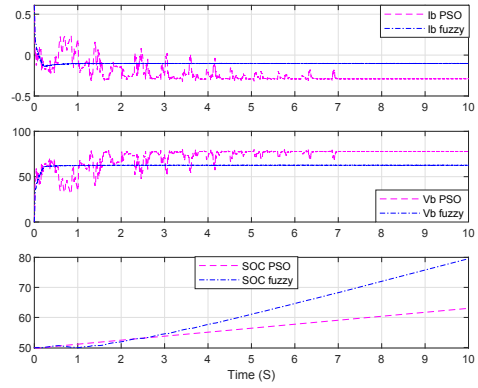

Fig. 14. The battery charge curve in case of PSC4

Chaibi, R., Yagoubi, M., and El Bachtiri, R. (2021). Robust dof control for uncertain polynomial fuzzy systems in finite frequency domain. *Results in Control and Optimization*, 5, 100062.

Chang, X.H. and Yang, G.H. (2010). Relaxed stabilization conditions for continuous-time takagi–sugeno fuzzy control systems. *Information Sciences*, 180(17), 3273–3287.

Chang, X.H., Zhang, L., and Park, J.H. (2015). Robust static output feedback h_∞ control for uncertain fuzzy systems. *Fuzzy Sets and Systems*, 273, 87–104.

Chouder, A. and Silvestre, S. (2009). Analysis model of mismatch power losses in pv systems. *J. Sol. Energy Eng*, 131, 024504–024509.

Dorofte, C., Borup, U., and Blaabjerg, F. (2005). A combined two-method mppt control scheme for grid-connected photovoltaic systems. In *2005 European Conference on Power Electronics and Applications*, 10–pp. IEEE.

Eberhart, R. and Kennedy, J. (1995). A new optimizer using particle swarm theory. In *MHS'95. Proceedings of the sixth international symposium on micro machine and human science*, 39–43. Ieee.

El Hammoumi, K., Chaibi, R., and El Bachtiri, R. (2022). Fuzzy state-feedback control for mppt of photovoltaic energy with storage system. *International Journal of Innovative Computing, Information and Control*, 18, 253–27.

Esram, T. and Chapman, P.L. (2007). Comparison of photovoltaic array maximum power point tracking techniques. *IEEE Transactions on energy conversion*, 22(2), 439–449.

Kumar, N., Hussain, I., Singh, B., and Panigrahi, B.K. (2017). Framework of maximum power extraction from solar pv panel using self predictive perturb and observe algorithm. *IEEE Transactions on Sustainable Energy*, 9(2), 895–903.

Mei, Q., Shan, M., Liu, L., and Guerrero, J.M. (2010). A novel improved variable step-size incremental-resistance mppt method for pv systems. *IEEE transactions on industrial electronics*, 58(6), 2427–2434.

Mekhilef, S., Safari, A., Mustaffa, W., Saidur, R., Omar, R., and Younis, M. (2012). Solar energy in malaysia: Current state and prospects. *Renewable and Sustainable Energy Reviews*, 16(1), 386–396.

Miyatake, M., Toriumi, F., Endo, T., and Fujii, N. (2007). A novel maximum power point tracker controlling several converters connected to photovoltaic arrays with particle swarm optimization technique. In *2007 European conference on power electronics and applications*, 1–10. IEEE.

Motahhir, S., El Hammoumi, A., and El Ghzizal, A. (2018). Photovoltaic system with quantitative comparative between an improved mppt and existing inc and p&o methods under fast varying of solar irradiation. *Energy Reports*, 4, 341–350.

Noguchi, T., Togashi, S., and Nakamoto, R. (2002). Short-current pulse-based maximum-power-point tracking method for multiple photovoltaic-and-converter module system. *IEEE Transactions on Industrial electronics*, 49(1), 217–223.

Phimmasone, V., Kondo, Y., Shiota, N., and Miyatake, M. (2013). The effectiveness evaluation of the newly improved pso-based mppt controlling multiple pv arrays. In *2013 1st International Future Energy Electronics Conference (IFEEC)*, 81–86. IEEE.

Shenoy, P.S., Kim, K.A., Johnson, B.B., and Krein, P.T. (2012). Differential power processing for increased energy production and reliability of photovoltaic systems. *IEEE Transactions on Power Electronics*, 28(6), 2968–2979.

Solangi, K., Islam, M., Saidur, R., Rahim, N., and Fayaz, H. (2011). A review on global solar energy policy. *Renewable and sustainable energy reviews*, 15(4), 2149–2163.

Takagi, T. and Sugeno, M. (1985). Fuzzy identification of systems and its applications to modeling and control. *IEEE transactions on systems, man, and cybernetics*, (1), 116–132.

Woyte, A., Nijs, J., and Belmans, R. (2003). Partial shadowing of photovoltaic arrays with different system configurations: literature review and field test results. *Solar energy*, 74(3), 217–233.

Zayani, H., Allouche, M., Kharrat, M., and Chaabane, M. (2015). T-s fuzzy maximum power point tracking control of photovoltaic conversion system. In *2015 16th International Conference on Sciences and Techniques of Automatic Control and Computer Engineering (STA)*, 534–539. IEEE.